Journal of Alloys and Compounds 572 (2013) 192–198

Contents lists available at SciVerse ScienceDirect

Journal of Alloys and Compounds

journal homepage: www.elsevier.com/locate/jalcom

Effect of particle size on the magneto-caloric properties of $Ni_{51}Mn_{34}In_{14}Si_1$ alloy

Rahul Das *, A. Perumal, A. Srinivasan

Department of Physics, Indian Institute of Technology Guwahati, Guwahati 781039, India

ARTICLE INFO

Article history:
Received 5 February 2013
Received in revised form 18 March 2013
Accepted 20 March 2013
Available online 02 April 2013

Keywords:
Magnetically ordered materials
Magneto-caloric effect
Ferromagnetic shape memory alloy
Milled powders
Particle size
Phase transitions

ABSTRACT

We have systematically investigated the effect of particle size on the magneto-caloric properties of $Ni_{51}Mn_{34}In_{14}Si_1$ alloy. Arc melted $Ni_{51}Mn_{34}In_{14}Si_1$ alloy was milled to reduce the average particle size and then vacuum annealed to reduce the strain accumulated in the particles during milling. Annealed particles were sieved and magneto-caloric parameters of the particles of different size ranges were systematically measured. It was observed that with decreasing particle size, the magnetic entropy change (ΔS_M) decreased but the refrigerant capacity (*RC*) increased to a maximum value and then decreased. The investigations reveal that the magneto-caloric parameters could be tuned over a wide range by changing the particle size of the alloy. *RC* (ΔS_M) obtained is 40.4 J kg^{-1} (11.2 J kg^{-1} K^{-1}) for the alloy with particle size ranging between 600 μm and 710 μm for an applied magnetic field change of 1.2 Tesla. These combined values of ΔS_M and *RC* are the highest reported for any ferromagnetic shape memory alloy particle. These studies indicate that $Ni_{51}Mn_{34}In_{14}Si_1$ alloy particles with controlled particle size are potential candidates for magnetic refrigeration near room-temperature.

1. Introduction

Magneto-caloric effect (MCE) which means heating up or cooling down of magnetic materials by an applied magnetic field was first observed by Warburg in 1881 in iron [1]. Later, Giauque and Debye independently explained this phenomenon and suggested its application in magnetic refrigeration [2,3]. MCE is generally measured in terms of isothermal entropy change (ΔS_M) or adiabatic temperature change (ΔT_{ad}) in a magnetic material when it is subjected to a magnetic field. If $\Delta S_M < 0$ (or $\Delta T_{ad} > 0$), the sample heats up upon application of magnetic field (direct MCE). On the other hand, if $\Delta S_M > 0$ (or $\Delta T_{ad} < 0$), the sample cools down when the external magnetic field is applied (inverse MCE) [4]. The current interest in these magnetic refrigerants is due to their environment friendly and energy saving attributes as compared to the gas-compression/expansion technology currently used in commercial refrigeration [5]. For commercial exploitation, the new technology materials exhibiting large MCE parameters such as ΔS_M (or ΔT_{ad}) and refrigerant capacity (*RC*) near room temperature for relatively low magnetic field change (ΔH) are required. Generally, ferromagnetic shape memory alloys (FSMAs) show two characteristic temperature induced phase transitions: a magnetic second-order phase transition at the Curie temperature (T_C) of the austenitic and martensite phases, and a structural first-order phase transition at the martensitic temperature (M_s), accompanied by a change in magnetization (ΔM) [6–15]. These FSMAs exhibit compositionally tunable magnetic, electric and structural properties which are important for various technological applications such as shape memory devices [16], magneto-resistive devices [17,18], magnetic field induced actuators [19], and especially, as regenerators in prototype magnetic refrigerators. The latest candidates of FSMAs are Ni–Mn–Sn and Ni–Mn–In based materials of which the characteristic temperatures were first reported by Sutou et al. [6]. Since then, melt-spun ribbons [20–24] and thin films [25,26] of Ni–Mn–In(Sn) alloys have also been studied. Oikawa et al. [8] reported a ΔS_M of 13 J kg^{-1} K^{-1} at M_S (190 K) in bulk $Ni_{46}Mn_{41}In_{13}$ alloys for a high ΔH of 9 T.

It is well known that the properties of FSMAs are sensitive to even a small change in composition. Exploiting this feature, several studies [27–31] of MCE in this alloy system has been carried out. These studies revealed that FSMAs exhibit very large MCE when a sharp change in magnetization occurs with a martensitic phase transformation [9,13]. Typically, $Ni_{50}Mn_{50-x}In_x$ alloys display maximum *RC* of 280 J kg^{-1} and 260 J kg^{-1} corresponding to ΔS_M of −6.8 J kg^{-1} K^{-1} and 23 J kg^{-1} K^{-1} near T_C and M_S, respectively, under ΔH of 5 T [27]. For the same ΔH, the *RC* (ΔS_M) as large as 279 J kg^{-1} (33 J kg^{-1} K^{-1}) has been obtained in $Ni_{47}Mn_{38}In_{15}$ alloy at 285 K [29]. In order to obtain high values of the MCE parameters, most of the investigators have used very high applied magnetic field (>2 T). Since such high fields restrict the commercial viability of these materials, attempts are being made to develop materials

* Corresponding author. Tel.: +91 361 2582743; fax: +91 361 2690762.
E-mail address: d.rahul@iitg.ernet.in (R. Das).

0925-8388/$ - see front matter © 2013 Elsevier B.V. All rights reserved.
http://dx.doi.org/10.1016/j.jallcom.2013.03.235

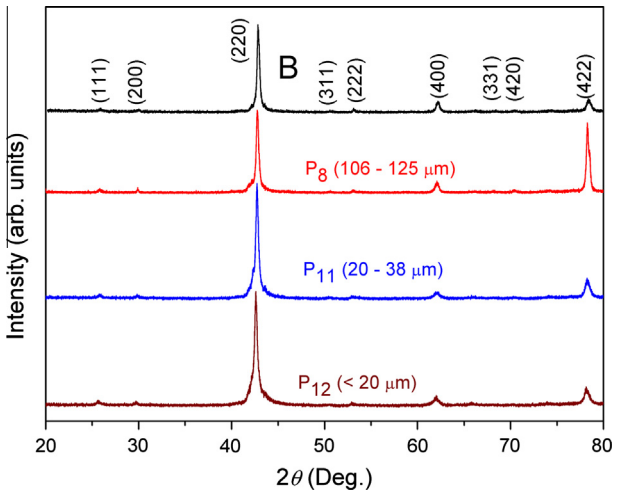

Fig. 1. Room temperature XRD patterns of bulk and three sets of $Ni_{51}Mn_{34}In_{14}Si_1$ powders with different average particle size (d_{av}).

which exhibit high ΔS_M and *RC* at lower amenable magnetic fields. For ΔH of 1T Han et al. [32] obtained high *RC* ($\sim$60 J kg^{-1}) in $Ni_{45.4}Mn_{41.5}In_{13.1}$ alloy with a peak ΔS_M of 8 J kg^{-1} K^{-1} and in case of melt spun ribbons Guan et al. [33] showed *RC* of 42.05 J kg^{-1} with very low ΔS_M (3.9 J kg^{-1} K^{-1}) for $Ni_{48}Co_2Mn_{35}In_{15}$ compound. Recently, Ni–Mn–In–Si alloys have been reported to possess excellent magneto-caloric properties at low field [34–36]. Santanna et al. [37] have demonstrated that particle size refinement can enhance *RC* despite reducing ΔS_M. These reports suggest that particle size refinement of a FSMAs composition exhibiting very high ΔS_M can provide a means to tailor its ΔS_M and *RC* to required values suitable for magnetic refrigerant application for reasonably low magnetic field change. However, no systematic studies on the effect of particle size over a wide range of particle sizes are available in the literature. In addition, it is important to note that for commercial exploitation of these magnetic refrigerants, large *RC* and ΔS_M near room temperature for viable magnetic fields (<2 T) are required. This motivated us to perform a systematic investigation of the structural phase transition, magnetic phase transition and magneto-caloric properties of $Ni_{51}Mn_{34}In_{14}Si_1$ alloy with different particle sizes.

2. Experimental

Polycrystalline $Ni_{51}Mn_{34}In_{14}Si_1$ alloy ingot was prepared by arc melting high purity (99.99%) elements. To counter preferential loss of Mn during arc-melting, an excess amount (1.2 wt.%) of Mn was taken. After melting several times, weight loss in the ingot was less than 1.5%. The ingot was sealed in a fused silica ampoule under a pressure of 10^{-3} Pa and annealed at 1173 K for 20 h and then quenched in ice water. The annealed ingot was crushed into particles of size <3 mm and milled for 7 h in a planetary ball mill (Insmart make). Hardened steel vial and hardened steel balls were used and 10:1 ball-to-powder weight ratio was maintained during the milling process. The mill was operated at a constant speed of 500 rpm. To avoid overheating of the vial, milling was carried out in cycles of 15 min followed by 10 min of idling. As-milled powders were subjected to the same heat treatment as the original ingot to minimize the strains accumulated during the milling process. Subsequently, the annealed powder was sieved using different pore sized metallic sieves conforming to ASTM standards and classified into different particle size ranges. The alloy powders studied are classified into thirteen sets depending on their size as B (bulk), P_1 (850–1180 μm), P_2 (710–850 μm), P_3 (600–710 μm), P_4 (500–600 μm), P_5 (425–500 μm), P_6 (300–425 μm), P_7 (125–300 μm), P_8 (106–125 μm), P_9 (90–106 μm), P_{10} (38–45 μm), P_{11} (20–38 μm), and P_{12} (<20 μm). A part of the sorted samples were used for structural analysis using a high power X-ray diffractometer (Rigaku TTRAX 18 kW) using Cu Kα radiation (λ = 0.15406 nm). Structural parameters of the samples were obtained from Rietveld analysis of the X-ray diffraction (XRD) patterns. Composition and particle sizes of the powders were verified using an energy dispersive spectrometer (EDS) attached to a scanning electron microscope (SEM, Leo 1430VP). Phase transition temperatures and the magnetization measurements as a function of temperature and magnetic field were performed using a vibrating sample magnetometer (VSM, Lakeshore 7410) equipped with a variable temperature (20–320 K) attachment. Magnetic moment calibration was performed with standard Ni sphere, prior to the magnetization measurements. Isothermal magnetization $(M–H)_T$ data were recorded at different temperatures as a function of increasing magnetic field from 0 to 1.2 T and decreasing temperature at 2 K interval. The measurement temperature was reached by cooling the sample from above the austenite finish temperature at zero magnetic fields and the measurements were made after allowing for stabilization of temperature. Heat capacity data at zero magnetic field were obtained using a physical properties measurement system (PPMS, Quantum Design).

3. Results and discussion

Fig. 1 depicts the room temperature XRD patterns of the heat treated bulk and three sets of sorted $Ni_{51}Mn_{34}In_{14}Si_1$ alloy powders. All the samples exhibit the cubic $L2_1$ structure corresponding to $Fm\bar{3}m$ space group of austenite phase. No additional (martensite or impurity) phases were found in the XRD patterns. The $L2_1$ structure is identified by the characteristic (1 1 1) and (3 1 1) peaks. In case of X_2YZ type compound Szytula et al. [38] have shown that the reflections with non-zero structure factors are obtained for the $L2_1$ structure when all indices are either even or odd. For first three reflections, the structure factors are $F(1\,1\,1) = 4(f_y - f_z)$, $F(2\,0\,0) = 4[2f_x - (f_y + f_z)]$, and $F(2\,2\,0) = 4[2f_x + f_y + f_z]$, where f_x, f_y and f_z are average scattering amplitudes for respective sub-lattices *X*, *Y* and *Z*. Any intermixing between *Y* and *Z* atoms can lead to the disordered B2 structure with the absence of $F(1\,1\,1)$ and reflections with all odd indices. Rietveld analysis of the XRD patterns reveal that alloy particles with sizes larger than 106 μm have the same unit cell dimension with lattice constant $a = 0.5974 \pm 0.0002$ nm.

Table 1
Space group, Wyckoff positions, particle size, measured alloy composition, lattice parameters (*a*, *b* and *c*), unit cell volume (*V*), and microstrain obtained for bulk and milled $Ni_{51}Mn_{34}In_{14}Si_1$ alloy.

Space group $Fm\bar{3}m$	Wyckoff positions In (0, 0, 0); Si (0, 0, 0); Mn (0, 0, 0) and (1/2, 1/2, 1/2); Ni (1/2, 1/2, 1/2) and (1/4, 1/4, 1/4).				
Alloy ID	Particle size, d_{av} (μm)	Composition from EDS	$a = b = c$ (nm)	V(nm)^3	Microstrain × 10^{-2} (%)
B	Bulk	$Ni_{50.69}Mn_{33.83}In_{14.07}Si_{1.41}$	0.5974	0.2132	25.9
P_1	850–1180	$Ni_{50.72}Mn_{33.89}In_{14.00}Si_{1.39}$	0.5974	0.2132	26.1
P_2	710–850	$Ni_{50.65}Mn_{33.85}In_{14.10}Si_{1.40}$	0.5974	0.2132	26.1
P_3	600–710	$Ni_{50.68}Mn_{33.90}In_{14.06}Si_{1.36}$	0.5974	0.2132	26.2
P_4	500–600	$Ni_{50.74}Mn_{33.91}In_{14.03}Si_{1.32}$	0.5974	0.2132	26.3
P_5	425–500	$Ni_{50.66}Mn_{33.80}In_{14.12}Si_{1.42}$	0.5974	0.2132	26.5
P_6	300–425	$Ni_{50.69}Mn_{33.89}In_{14.00}Si_{1.42}$	0.5974	0.2132	27.0
P_7	125–300	$Ni_{50.67}Mn_{33.85}In_{14.07}Si_{1.41}$	0.5974	0.2132	27.3
P_8	106–125	$Ni_{50.70}Mn_{33.87}In_{14.09}Si_{1.34}$	0.5974	0.2132	28.9
P_9	90–106	$Ni_{50.72}Mn_{33.88}In_{14.00}Si_{1.40}$	0.5975	0.2132	32.5
P_{10}	38–45	$Ni_{50.67}Mn_{33.83}In_{14.09}Si_{1.41}$	0.5977	0.2133	41.8
P_{11}	20–38	$Ni_{50.68}Mn_{33.84}In_{14.08}Si_{1.40}$	0.5981	0.2140	52.4
P_{12}	<20	$Ni_{50.71}Mn_{33.85}In_{14.02}Si_{1.42}$	0.5992	0.2151	68.9